Evidence for Bending of a Nitrosyl Group during One-Electron Reduction of Cyclopentadienyl Metal Nitrosyl Compounds†

William E. Geiger,*‡ Philip H. Rieger,*§ Bunchai Tulyathan,‡ and Marvin D. Rausch⊥

Contribution from the Departments of Chemistry, University of Vermont, Burlington, Vermont 05405, Brown University, Providence, Rhode Island 02912, and University of Massachusetts, Amherst, Massachusetts 01003. *Received November 10, 1983*

Abstract: Electrochemical reduction of $CpM(CO)_2(NO)$, M = Cr, Mo, occurs as an ECE mechanism in nonaqueous solvents. The initial one-electron reduction gives a radical anion with a half-life of ca. 1 s at 298 K. The charge transfer is quasireversible with a k_s value of ca. $1-2 \times 10^{-2}$ cm/s^{-1}. Frozen and fluid solutions of the radical anions were studied by ESR spectroscopy, and a non-coincidence of the **g** tensor and hyperfine axes of 105–110° was revealed. ESR parameters are consistent with the extra electron being localized in the M–N–O group and with the metal nitrosyl group being bent as a consequence of the reduction.

Structural conversion of a metal nitrosyl from a linear to a bent form is an attractive way to generate a coordinatively unsaturated metal since bending changes the nitrosyl from a 3 e$^-$ to a 1 e$^-$ donor ligand:[1]

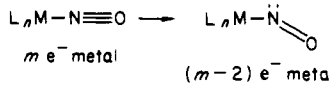

Electron-rich metals (e.g., >18 e$^-$) might relieve the electronic "strain" by donating electrons to the nitrogen sp^2 orbital and bending of the M–N–O bond could accompany this process. The connection between electronic structure and geometry of the MNO group is established,[2-5] and indeed most bent nitrosyls are attached to electron-rich metals.[6] Reduction of a metal nitrosyl compound therefore may facilitate the linear-to-bent structural change in addition to leading to a more nucleophilic nitrosyl group.[7,8] Redox studies on M–N–O coordination compounds[8-20] have shown that reduction may irreversibly labilize one of the ligands[9,13] or (more often) involve reversible electron transfer to a molecular orbital based predominantly on the nitrosyl group,[15] on another ligand,[18,19] or on the metal.[21]

In contrast, reports of reversible redox processes for organometallic nitrosyl compounds are surprisingly rare. Chemically reversible reductions have been reported for $Co(NO)(CO)_3$,[22] $(allyl)Fe(NO)(CO)_2$,[23] $Fe(NO)_2(CO)_{2-x}L_x$,[25] CpNi(NO) (Cp = η^5-C_5H_5),[26] $CpW(CO)_2(NO)$,[27] and $CpMn(CO)_2(NO)^+$.[28] Except for compounds involving bridging nitrosyls,[29-32] only the organometallic dithiolates $CpMn(S_2C_2R_2)(NO)$[33-35] and the dinitrosyl cations $CpW(NO)_2(PR_3)^+$[36] have been reported to undergo reversible redox processes.

In this paper we report the chemically reversible reduction of the complexes $CpM(CO)_2(NO)$, M = Cr or Mo, **1-3**. The electrochemical and electron spin resonance data strongly suggest that the electron transfers into an orbital which is essentially M–NO σ^* in character and that severe bending of the MNO bond accompanies the electron-transfer process.

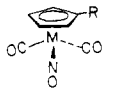

1, M = Cr; R = H
2, M = Cr; R = COMe
3, M = Mo; R = H

Experimental Section

Chemicals. Compounds **1-3** were prepared according to published methods.[37] As solids they can be handled for brief periods in air, but their solutions are air sensitive. We obtained some electrochemical data (e.g., dc polarography) using nitrogen-blanketing procedures, but most

† Structural Consequences of Electron-Transfer Reactions. 10. Part 9: Edwin, J.; Geiger, W. E.; Rheingold, A. L. *J. Am. Chem. Soc.* **1984**, *106*, 3052.

‡ University of Vermont.

§ Brown University.

⊥ University of Massachusetts.

(1) Schoonover, W. M.; Baker, E. C.; Eisenberg, R. *J. Am. Chem. Soc.* **1979**, *101*, 1880 and references therein.
(2) Enemark, J. H.; Feltham, R. D. *Coord. Chem. Rev.* **1974**, *13*, 339.
(3) Hoffmann, R.; Chen, M. M. L.; Elian, M.; Rossi, A. R.; Mingos, D. M. P. *Inorg. Chem.* **1974**, *13*, 2666.
(4) Pierpont, C. G.; Eisenberg, R. *J. Am. Chem. Soc.* **1971**, *93*, 4905.
(5) Hawkins, T. W.; Hall, M. B. *Inorg. Chem.* **1980**, *19*, 1735.
(6) Feltham, R. D.; Enemark, J. H. "Topics in Inorganic and Organometallic Stereochemistry", Geoffroy, G. L., Ed.; John Wiley and Sons: New York, 1981; p 155.
(7) Bottomley, F. *Acc. Chem. Res.* **1978**, *11*, 158.
(8) Masek, J. *Inorg. Chim. Acta. Rev.* **1969**, *3*, 99.
(9) Bowden, W. L.; Bonnar, P.; Brown, D. B.; Geiger, W. E. *Inorg. Chem.* **1977**, *16*, 41.
(10) Masek, J.; Maslova, E. *Collect. Czech. Chem. Commun.* **1974**, *39*, 2141.
(11) Armour, J. N.; Hoffman, M. Z. *Inorg. Chem.* **1975**, *14*, 444.
(12) Bustin, D. I.; Vlcek, A. A. *Collect. Czech. Chem. Commun.* **1967**, *32*, 1665.
(13) Masek, J.; Pribil, R. *Inorg. Chim. Acta* **1970**, *4*, 175.
(14) Dessy, R. E.; Charkoudian, J. C.; Rheingold, A. L. *J. Am. Chem. Soc.* **1972**, *94*, 738.
(15) Callahan, R. W.; Brown, G. M.; Meyer, T. J. *J. Am. Chem. Soc.* **1975**, *97*, 894.
(16) Keene, F. R.; Salmon, D. J.; Meyer, T. J. *J. Am. Chem. Soc.* **1977**, *99*, 4821.
(17) Keene, F. R.; Salmon, D. J.; Walsh, J. L.; Abruna, H. D.; Meyer, T. J. *Inorg. Chem.* **1980**, *19*, 1896.
(18) McCleverty, J. A.; Atherton, N. M.; Locke, J.; Wharton, E. J.; Winscom, C. J. *J. Am. Chem. Soc.* **1967**, *89*, 6082.
(19) McCleverty, J. A.; Atherton, N. M.; Connelly, N. G.; Winscom, C. J. *J. Chem. Soc. A* **1969**, 2242.
(20) Budge, J. R.; Broomhead, J. A.; Boyd, P. D. W. *Inorg. Chem.* **1982**, *21*, 1031.
(21) Sweeney, W. V.; Coffman, R. E. *J. Phys. Chem.* **1972**, *76*, 49.
(22) Piazza, G.; Foffani, A.; Paliani, G. *Z. Phys. Chem. (Frankfurt/Main)* **1968**, *60*, 167.
(23) Paliani, G.; Murgia, S. M.; Cardaci, G. *J. Organomet. Chem.* **1971**, *30*, 221.
(24) Piazza, G.; Paliani, G. *Z. Phys. Chem. (Frankfurt/Main)* **1970**, *71*, 91.
(25) Pribil, R.; Masek, J.; Vlcek, A. A. *Inorg. Chim. Acta* **1971**, *5*, 57.
(26) Paliani, G. *Z. Naturforsch. B* **1970**, *25B*, 786.
(27) Dessy, R. E.; King, R. B.; Waldrop, M. *J. Am. Chem. Soc.* **1966**, *88*, 5112.
(28) Dessy, R. E.; Stary, F. E.; King, R. B.; Waldrop, M. *J. Am. Chem. Soc.* **1966**, *88*, 471.
(29) Bernal, I.; Korp, J. D.; Reisner, G. M.; Herrmann, W. A. *J. Organomet. Chem.* **1977**, *139*, 321.
(30) Clamp, S.; Connelly, N. G.; Payne, J. D. *J. Chem. Soc., Chem. Commun.* **1981**, 897.
(31) Connelly, N. G.; Payne, J. D.; Geiger, W. E. *J. Chem. Soc., Dalton Trans.* **1983**, 295.
(32) Clamp, S.; Connelly, N. G.; Payne, J. D.; Geiger, W. E., unpublished results.

0002-7863/84/1506-7000$01.50/0

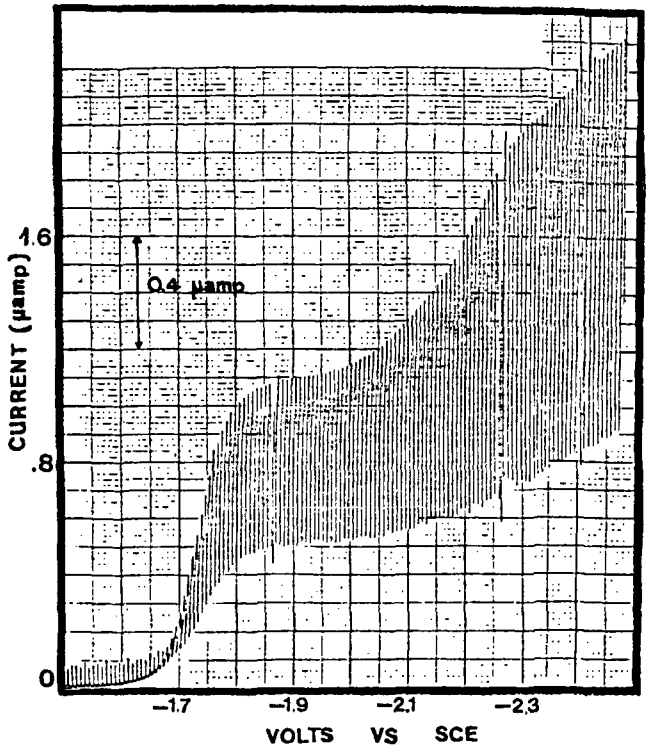

Figure 1. Direct current polarogram of $CpMo(CO)_2(NO)$ in THF/Bu_4NPF_6.

experiments were conducted in a drybox (Vacuum Atmospheres). Dimethylformamide, DMF (Fisher Spectrograde), was vacuum distilled from CaH_2 or treated with molecular sieves without distillation when Burdick and Jackson was the supplier, with equivalent results. Tetrahydrofuran, THF (Aldrich Goldlabel), was vacuum distilled, first from $LiAlH_4$ and then from benzophenone ketyl. Acetonitrile (Aldrich Spectrograde) was distilled from CaH_2. Tetrabutylammonium hexafluorophosphate was prepared by metathesis of Bu_4NI (Eastman) and ammonium hexafluorophosphate (Ozark Mahoning) in acetone, followed by addition of water. It was recrystallized twice from 95% ethanol and vacuum dried. Tetraethylammonium perchlorate (Southwestern Analytical Chemicals) was recrystallized from water and vacuum dried.

Physical Measurements. The electrochemical instrument was a Princeton Applied Research Model 173 potentiostat with Model 176 digital coulometer and Model 179 waveform generator. Recordings were made on either a Hewlett-Packard Model 70001A x-y recorder or a Tektronix Model 564 storage oscilloscope. The reference electrode was an aqueous saturated calomel electrode (SCE), which was separated from the test solutions by an agar bridge and a fine frit. Further details on the voltammetric measurements are as previously given.[38] ESR data were recorded on either an X-band spectrometer, Varian V-4502, at the University of Vermont, or a Q-band instrument at the University of New Hampshire. Spectra were calibrated by using the diphenylpicrylhydrazyl radical (g = 2.0036) in a dual-cavity arrangement: frozen solution spectra were analyzed by a non-linear least-squares procedure[39] and simulated by using the computer program of Peake et al.[40]

Results

Electrochemistry. Electrochemical behavior of the three compounds was quite similar. Each undergoes two reductions, only the first of which demonstrates any reversibility. Voltammetric behavior was independent of the electrode material (Pt or Hg)

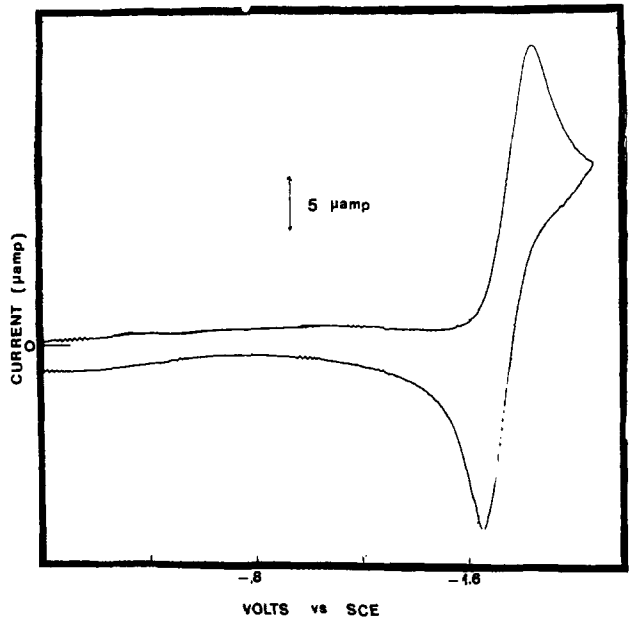

Figure 2. Cyclic voltammogram at v = 300 mV s^{-1} for the first reduction of $CpMo(CO)_2(NO)$ in DMF/Bu_4NPF_6 at 233 K (platinum electrode).

and displayed only minor changes (detailed below) in different solvents (CH_3CN, DMF, THF). The discussion centers on the behavior of **3**, as representative of the group of compounds, in polarographic (dc and ac), cyclic voltammetric, and bulk coulometric experiments.

Direct current (dc) polarograms of $CpMo(CO)_2NO$ in THF revealed two reduction waves with $E_{1/2}$ values of −1.73 and −2.20 V (Figure 1). The first reduction of the chromium compound **1** occurred at a slightly more negative voltage, $E_{1/2}$ = −1.83 V, but that of **2** was considerably more facile, $E_{1/2}$ = −1.53 V, reflecting the electron-withdrawing effect of the acetyl group. A third wave ($E_{1/2}$ = −2.50 V) for **3** which arises from the products of the irreversible second reduction was not studied. Our attention focused on the first wave with the specific purpose of investigating the existence and properties of a radical anion generated in that step.

The one-electron reduction of the neutral complex is not fully reversible in either the chemical or electrochemical sense. Cyclic voltammetry (CV) scans revealed some evidence of anion decomposition at slow scan rates, and evidence of quasireversibility in the *charge-transfer* step itself was found in the polarographic wave shape and in CV peak potential separations. The polarographic $-E_{app}$ vs. log $[i/(i_d - i)]$ slope was 74 mV, compared to the 59 mV expected for a one-electron reversible process,[41] and CV peak separations were about 80 mV under conditions in which we measured 65 mV for ferrocene. CV data were used to calculate heterogeneous charge-transfer rates for **1** and **3** (vide infra).

Slow sweep rate CV experiments or positive-going scans initiated negative of the first reduction wave showed irreversible product oxidation waves at E_{p_a} = −0.58 and −0.28 V for **3**. With a reduction in temperature these product waves were diminished and the reduction of the molybdenum compound appeared completely chemically reversible at 233 K (Figure 2). Bulk coulometric experiments to generate the anions were conducted in DMF or THF, since the radicals were somewhat more stable in these solvents than in CH_3CN.

Bulk electrolysis of **3** at 253 K in DMF at −1.9 V gave n = 1 by coulometry (n_{meas} = 1.1 e^-) and a brown-orange solution of the radical anion which was removed and frozen for ESR analysis. If the electrolysis was performed at ambient temperature, production of the anion was not as clean, judging by a higher coulomb count and smaller concentrations of anion radical shown by post-electrolysis CV scans. Thus, bulk coulometry in DMF at

(33) McCleverty, J. A.; James, T. A.; Wharton, E. J. *Inorg. Chem.* **1969**, *8*, 1340.
(34) McCleverty, J. A.; Orchard, D. G. *J. Chem. Soc. A* **1970**, 3315.
(35) Hydes, P.; McCleverty, J. A.; Orchard, D. G. *J. Chem. Soc. A* **1971**, 3660.
(36) Yu, Y. S.; Jacobson, R. A.; Angelici, R. J. *Inorg. Chem.* **1982**, *21*, 3106.
(37) Rausch, M. D.; Mintz, E. A.; Macomber, D. W. *J. Org. Chem.* **1980**, *45*, 689.
(38) Moraczewski, J.; Geiger, W. E. *J. Am. Chem. Soc.* **1981**, *103*, 4779.
(39) Reiger, P. H. *J. Magn. Reson.*, in press.
(40) Peake, B. M.; Reiger, P. H.; Robinson, B. H.; Simpson, J. *J. Am. Chem. Soc.* **1980**, *102*, 156.
(41) Meites, L. "Polarographic Techniques", 2nd ed.; Interscience Publishers: New York, 1965; Chapter 4.

297 K gave $n = 2.0$ e⁻ as the solution went from yellow to brown. The polarographic diffusion current constant, I, also increased with longer experiment (drop) times in THF, going from 3.1 at drop time = 0.5 s to 3.7 at 7 s (for comparison purposes, the one-electron oxidation of ferrocene gave $I = 3.0$). Finally, in CV experiments the cathodic current function[42] increased significantly as the scan rate was lowered. In comparing the current function of **3** with that of ferrocene, the **ratio** was 1.0 at a scan rate of $v = 900$ mV/s^{-1}, but it rose to 1.47 at $v = 20$ mV/s^{-1}. The increase in the apparent n value in longer voltammetry experiments and the $n_{app} = 2$ value measured by ambient temperature bulk coulometry are consistent with an ECE mechanism at the first wave, in which $\mathbf{3}^-$ reacts to form an unspecified product which is further reduced by one electron at the electrolysis potential. Attempts were made to identify the 2-electron reduction product(s). It (they) had oxidation waves at −0.6, −0.36, and −0.2 V. The relative heights and reversibility of these waves were dependent on the microelectrode used. Interestingly, some of the original compound could be regenerated if the reduced solution were re-electrolyzed at −0.1 V. In this reduction/reoxidation cycle about 20% of the original compound **3** was regenerated, the other product of this "re-cycling" having a reduction wave at −0.9 V. After bulk electrolytic reduction in CH_3CN/Et_4NClO_4 at −1.9 V, the product oxidation waves matched those seen after reduction in THF [−0.65 V (reversible) and −0.2 V (irreversible)]. The solvent was removed and the product extracted away from the supporting electrolyte with THF, giving a brown material (about 20% of the original weight) with IR activity in the carbonyl/nitrosyl region: 1910, 1780, 1690, 1605, 1557 cm^{-1}. This is probably a mixture of products, and purification was not pursued.

Electrochemical and Chemical Rate Constants from CV Data. The rate constant for the intervening chemical reaction in the ECE process (eq 2) at the first reduction wave was calculated from the scan rate dependence of the cathodic current function by using the method of Nicholson and Shain.[43] This was done to obtain a rate constant for the decomposition of the primary anion radical, $CpM(CO)_2(NO)^-$. In this method, the ratio of the current function[42] at a particular scan rate χ(kinetic) to that at the diffusion-controlled limit χ(diffusion) is used to obtain the ratio k_c/a from eq 1. In this equation, $a = nFv/RT$ and a first-order

$$\frac{\chi(\text{kinetic})}{\chi(\text{diffusion})} = \frac{0.400 + (k_c/a)}{0.396 + 0.47(k_c/a)} \quad (1)$$

or pseudo-first-order chemical reaction is assumed. The term χ(diffusion) refers to the current function under conditions in which the kinetics of the follow-up reaction are unimportant; in this case that is the fast-scan limit. χ(kinetic) is the current function at slower scan rates and contains the extra current due to the ECE process. In principle, data at only one scan rate in the "kinetic" region are needed to obtain the rate constant k_c, which refers to the rate of decomposition of the radical anion:

$$CpM(CO)_2NO \underset{E}{\overset{k_s}{\rightleftharpoons}} CpM(CO)_2NO^- \xrightarrow[C]{k_c} \text{electroactive product} \underset{E}{\rightleftharpoons} ? \quad (2)$$

However, it is more reliable to measure k_c/a at a number of scan rates and plot these values vs. $1/a$ to obtain k_c from the slope. Excellent correlations were obtained for scan rates in the range 25–400 mV/s. For $CpMO(CO)_2NO$ in THF this procedure gave $k_c = 0.80$ s^{-1} and a half-life of 0.9 s for the anion at 298 K; a rate constant of 0.85 s^{-1} was obtained for the chromium analogue (**1**). *Hence the rate of radical decomposition is essentially independent of the metal.* The rate constant decreased to 0.10 s^{-1} for **3** at 263 K (half-life = 7 s).

(42) The cathodic current function (ref 43) is proportional to $i_{p_c}/v^{1/2}$, where i_{p_c} is the peak cathodic current and v is the CV scan rate. For an uncomplicated diffusion-controlled charge transfer, it is independent of scan rate, and changes in the current function are diagnostic of kinetic contributions to the current due to occurrence of chemical reactions coupled to the charge-transfer step.

(43) Nicholson, R. S.; Shain, I. *Anal. Chem.* **1965**, *37*, 190.

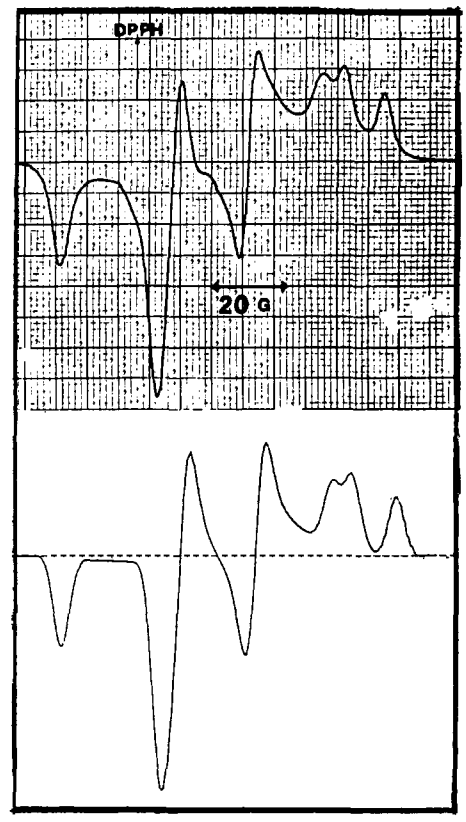

Figure 3. Experimental (upper) and simulated (lower) X-band ESR spectra of $CpCr(CO)_2NO^-$ in frozen DMF solution.

The standard heterogeneous rate constants, k_s, for electron transfer were also evaluated by cyclic voltammetry. Data were taken in DMF (to minimize solution resistance) at a platinum electrode and used in eq 3: the dimensionless parameter ψ was calculated from ΔE_p measurements at various scan rates and the ψ vs. ΔE_p working curve of Nicholson.[44] The diffusion coefficients

$$k_s = \psi(\pi a D_0)^{1/2} \quad (3)$$

D_0 were calculated from the polarographic diffusion current constants[45] in DMF ($D_0 = 2.1 \times 10^{-5}$ cm^2 s^{-1}). Over the range $v = 24$ to 730 mV/s^{-1}, values of $k_s = (1.2 \pm 0.2) \times 10^{-2}$ cm s^{-1} were obtained for both **1** and **3** on platinum. For the chromium compound **1**, a value of $k_s = 2.6 \times 10^{-2}$ cm s^{-1} was obtained on a mercury electrode in DMF. This value was calculated from phase-selective ac polarographic measurements at a dropping mercury electrode. The transfer coefficient α was calculated as 0.58 from these ac measurements.[46] The electron-transfer parameters establish that the charge-transfer step itself is a quasireversible process, relatively independent of the nature of the metal in the compound or the type of electrode surface.

Oxidation of $CpM(CO)_2(NO)$. Both **1** and **3** exhibit a multielectron irreversible oxidation wave at $e_{p_a} = +1.2$ V at a scan rate of 200 mV s^{-1}. The peak current for the $CpMo(CO)_2(NO)$ oxidation is about 3 times that of its reduction wave, and bulk oxidation resulted in release of 2.5 electrons per mol as the solution went from yellow to green. Several irreversible reduction waves due to uncharacterized products were present after completion of the electrolysis ($e_{p_c} = +0.02, -0.35, -0.71$ V).

Electron Spin Resonance. X-Band ESR spectra of $\mathbf{1}^-$ and $\mathbf{3}^-$, produced in DMF fluid solution at 223 K as described above, consist of the expected three lines due to hyperfine interaction of the unpaired electron with the ^{14}N nucleus of the nitrosyl group.

(44) Nicholson, R. S. *Anal. Chem.* **1965**, *37*, 1351.

(45) Heyrovsky, J.; Kuta, J. "Principles of Polarography"; Academic Press: New York, 1965; Chapter 6.

(46) Smith, D. E. In "Electroanalytical Chemistry", Bard, A. J., Ed.; Marcel Dekker: New York, 1966; Vol. 1, p 1.

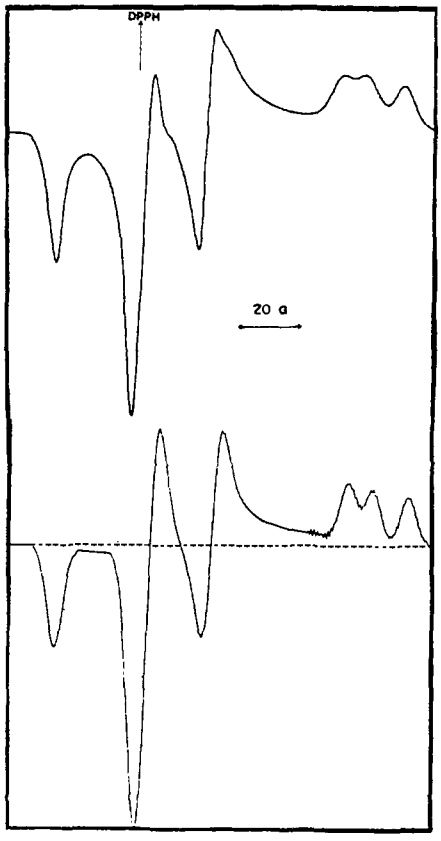

Figure 4. Experimental (upper) and simulated (lower) X-band ESR spectra of $CpMo(CO)_2NO^{\cdot}$ in frozen DMF solution.

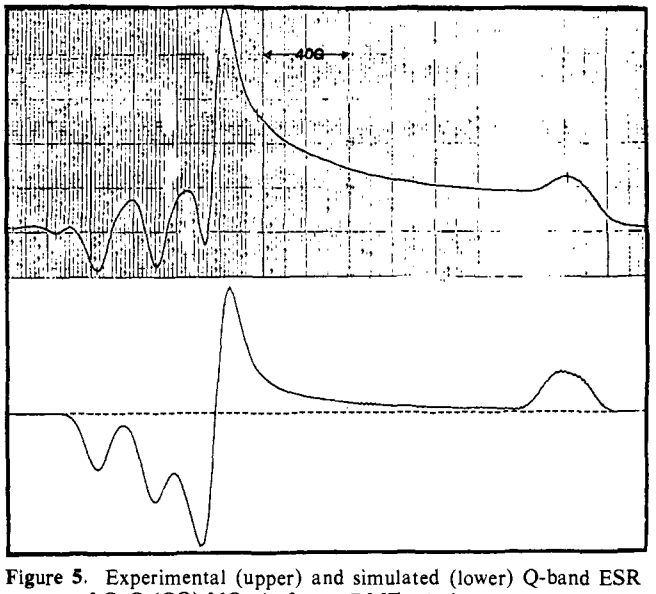

Figure 5. Experimental (upper) and simulated (lower) Q-band ESR spectra of $CpCr(CO)_2NO^{\cdot}$ in frozen DMF solution.

No chromium or molybdenum coupling was observed; upper limits of 9 and 6 G can be estimated for the isotopic ^{53}Cr and $^{95}Mo/^{97}Mo$ couplings, respectively.

X-Band ESR spectra of frozen DMF solutions of the radical anions of **1** and **3** are shown in Figures 3 (top) and 4 (top), and the Q-band spectrum of $\mathbf{1}^-$ is shown in Figure 5, top. To a first approximation, the spectra may be understood in terms of approximately axial **g** and hyperfine tensors with the "parallel" hyperfine axis corresponding to one of the "perpendicular" **g**-tensor axes. Thus the three low-field features correspond to the three $g_\perp$, $A_\parallel$ components; the $g_\perp$, $A_\perp$ components are unresolved and superimposed on the middle low-field feature. The three high-field features then correspond to $g_\parallel$ and $A_\perp$ (see Figure 6). Although this assignment explains the gross features of the spectra, it does

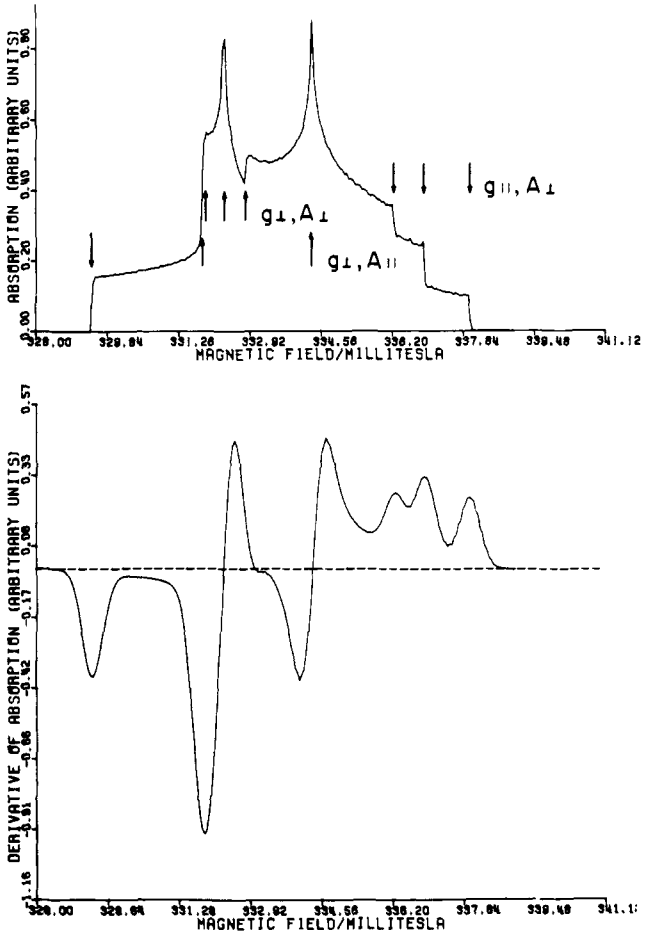

Figure 6. X-Band ESR absorption spectrum, simulated with zero line width, showing the positions of spectral features for $m_n = -1$, 0, and +1.

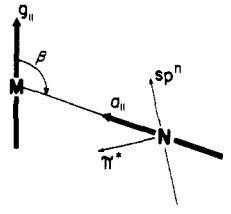

Figure 7. The angle β is defined by the $g_\parallel$ and $a_\parallel$ tensor axes. The $a_\parallel$ tensor axis is the major axis of the nitrogen 2p contribution to the SOMO; this contribution is a linear combination of NO sp^n and π^* orbitals.

not account for the uneven spacing of the three high-field lines; the spacings of these features in Figure 3 are about 7 and 13 G whereas second-order shifts lead to an expected spacing difference of only about 0.1 G.

A clue to the interpretation is found in the non-coincidence of the "parallel" axes of the **g** and hyperfine tensors. If the angle separating these axes (the Euler angle β, see Figure 7) is not zero, there is no reason that it should be exactly 90°. Accordingly, computer simulations of the spectrum were undertaken in which the angle β was varied. The computer program used to simulate the spectra was an extension of that described by Peake et al.;[40] the extension to the program algorithm is described elsewhere.[39]

The spacings of the $g_\parallel$, $A_\perp$ features and the resolution of the $g_\perp$, $A_\perp$ components proved to be strongly dependent on β, and it became apparent that the anomalies could be completely explained by an angle $\beta \cong 105$–$110°$ (or 70–75°). In practice, a least-squares procedure[39] was used to fit measured field positions of features in the X-band spectra to the g and hyperfine tensor components and the angle β. In applying the least-squares procedure, we allowed for complete anisotropy of the **g** tensor (g_1, g_2) $\cong g_\perp$, $g_3 = g_\parallel$) but assumed that the hyperfine tensor is exactly

Table I. Some Electrochemical Data for the First Reduction of $(C_5H_4R)M(CO)_2(NO)$

compound	solvent	polarography		cyclic voltammetry		
		$E_{1/2}$[a]	slope[b]	v[c]	ΔE_p[d]	i_a/i_c[e]
$CpCr(CO)_2(CO)$ (1)	THF	−1.83	69	70	86	0.98
				800	114	1.01
	DMF	−1.85	70	70	74	0.98
				800	111	1.04
$(C_5H_5COCH_3)Cr(CO)_2(NO)$ (2)	THF	−1.58	*f*	70	100	0.74
				800	102	0.90
	DMF	−1.50	*f*	70	60	0.97
				800	126	1.02
$CpMo(CO)_2(NO)$ (3)	THF	−1.73	74	70	85	1.00
				800	128	1.07
	DMF	−1.76	74	70	76	0.98
				800	150	1.04

[a] Volts vs. SCE. [b] Plot of $-E_{app}$ vs. log $[(i/(i_d - i)]$, in mV. [c] Scan rate in mV s^{-1}. [d] Separation between cathodic and anodic peaks, in mV. [e] Ratio of anodic to cathodic currents. [f] Not measured.

Table II. ESR Parameters

	$CpCr(CO)_2NO^{\cdot}$	$CpMo(CO)_2NO^{\cdot}$
$\langle g \rangle$	1.990 ± 0.002	1.992 ± 0.002
$\langle A \rangle$[a]	11.3 ± 0.2	9.7 ± 0.4
g_1[b]	2.001 ± 0.002	2.005 ± 0.002
g_2[b]	1.998 ± 0.002	2.002 ± 0.002
g_3[b]	1.971 ± 0.002	1.959 ± 0.002
$A_\parallel$[a]	24.5 ± 0.5	25.1 ± 0.5
$A_\perp$[a]	4.7 ± 0.5	2.0 ± 0.5
β, deg	104.6 ± 2.0	111.8 ± 2.0

[a] Units of 10^{-4} cm^{-1}. [b] Relative errors of the **g**-tensor components are ca. ±0.0005.

axial. We also required that the traces of the tensors be related to the isotropic parameters by eq 4. Thus with three constraints,

$$g_1 + g_2 + g_3 = 3\langle g \rangle \quad (4a)$$

$$A_\parallel + 2A_\perp = 3\langle A \rangle \quad (4b)$$

the seven parameters (three components of each tensor plus the angle) were reduced to four. The least-squares fit to seven observed spectral features then had three degrees of freedom permitting a rough estimate of the parameter standard deviations. These were used, together with estimated uncertainties in the experimental fields and microwave frequency, to obtain the error limits given in Table II. The parameters of Table II were used to simulate the spectra shown in Figures 3 (bottom), 4 (bottom), 5 (bottom), and 6. The match between experiment and simulation is very good. The high-field features are not resolved in the experimental Q-band spectrum so that the fit in this case is not very sensitive to $A_\perp$ or to the angle β. The good agreement between the experimental and simulated Q-band spectra, however, does confirm the **g**-tensor assignments.

Interpretation of ESR Parameters. The nitrogen hyperfine parameters, $A_\parallel$, $A_\perp$, and A, all have the same sign which we assume is positive. Neglecting spin–orbit contributions, which should be negligible for nitrogen, the dipolar coupling of the ^{14}N nucleus with electron spin density on nitrogen[47] may be obtained from

$$b_\parallel = A_\parallel - \langle A \rangle \quad (5a)$$

$$b_\perp = A_\perp - \langle A \rangle \quad (5b)$$

where

$$b_\parallel = -2b_\perp = {}^4/_5 P \rho_p^N \quad (6)$$

P is the nitrogen 2 p dipolar coupling parameter and ρ_p^N is the nitrogen 2p spin density. With $P = 46.3 \times 10^{-4}$ cm^{-1},[49] ρ is 0.36 and 0.39 for the radical anions of 1 and 3, respectively. The isotopic nitrogen coupling is more difficult to interpret as it arises both from direct contribution of nitrogen 2s character to the semioccupied molecular orbital (SOMO), a positive contribution to $\langle A \rangle$, and from polarization of filled molecular orbitals with 1s or 2s character, a negative contribution. A single nitrogen 2s electron is expected to give a coupling of 604×10^{-4} cm^{-1},[49] suggesting a minimum 2s contribution of about 0.02. When polarization contributions to $\langle A \rangle$ are taken into account, the 2s contribution to the SOMO may be larger, possibly by as much as a factor of 2 or 3. Even so, the nitrogen contribution to the SOMO is largely 2p.

Nitrogen contributions to the SOMO account for about 40% of the spin density. Although there may be some spin density on the nitrosyl oxygen,[50] the metal contribution must be substantial since the **g**-tensor anisotropy increases significantly when Cr is replaced by Mo. The **g**-tensor components are given by[54]

$$g_i = g_e + \lambda \sum_{k \neq 0} \frac{|\langle 0|L_i|k\rangle|^2}{E_0 - E_k} \quad (7)$$

where λ is the spin–orbit coupling parameters ($\lambda_{Mo} > \lambda_{Cr}$) and $E_0 - E_k$ is the energy difference between the SOMO and the kth MO. The only significant deviation from the free-electron **g** value, $g_3 < g_e$, implies the existence of one or more low-lying empty MO's, $E_0 < E_k$, which are coupled to the SOMO by one (only) of the component angular momentum operators, $\hat{L}_3$.

Reasoning from the ESR parameters alone, we cannot proceed much further. Although we know the relative orientation of the major axes of the **g** and ^{14}N hyperfine tensors, we do not know the position of either axis in a molecular coordinate system; thus the angle β by itself is not very useful. We turn then to the results of molecular orbital theory to build a model consistent with the ESR parameters.

The SOMO and the M–N–O Angle. In a d^6 $CpM(CO)_3$ complex of pseudo-C_{3v} symmetry, the LUMO is[55]

$$\psi_1 = N_1(d_{x^2-y^2} - R_1 d_{xz}) \quad (8a)$$

$$\psi_2 = N_2(d_{xy} + R_2 d_{yz}) \quad (8b)$$

The hybridization ratios R_1 and R_2 depend strongly on the OC–M–CO bond angles, and for 90° angles, $R_1 = R_2 = 2^{1/2}$. When

(47) A small contribution from the dipolar interaction between the ^{14}N nucleus and spin density on the metal[48] can be neglected here without serious error.

(48) Goodman, B. A.; Raynor, J. B.; Symons, M. C. R. *J. Chem. Soc. A* **1969**, 2572.

(49) Morton, J. R.; Preston, K. F. *J. Magn. Reson.* **1978**, *30*, 577.

(50) By analogy, organic nitroxides always show substantial spin density on both N and O. This can be deduced from the observed ^{17}O and ^{14}N splittings in di-*sec*-butyl nitroxide (13.4 and 19.7 G, respectively)[51] and σ-polarization constants for those two nuclei.[52,53]

(51) Baird, J. C. *J. Chem. Phys.* **1962**, *37*, 1879.

(52) Ayscough, P. B. "Electron Spin Resonance in Chemistry"; Methuen and Co.: London, 1967; p 270.

(53) Broze, M.; Luz, Z.; Silver, B. L. *J. Chem. Phys.* **1967**, *46*, 4891.

(54) Atherton, N. M. "Electron Spin Resonance"; Ellis Horwood: Chichester, England, 1973.

(55) Lichtenberger, D. L.; Fenske, R. F. *J. Am. Chem. Soc.* **1976**, *98*, 50–63.

one of the CO ligands is replaced by NO, the degeneracy is lifted, and assuming C_s symmetry, eq 8a and 8b belong to the a′ and a″ representations, respectively. Both orbitals are metal–ligand antibonding, but with respect to the NO ligand, the a′ orbital has approximate σ^* symmetry while the a″ orbital is metal–nitrogen π^*. In the radical anions of **1** and **3**, we expect one of these orbitals to be the SOMO, the other a low-lying empty orbital.

In $\{MNO\}^8$ square-pyramidal nitrosyl complexes,[56] e.g., $IrCl_2(NO)(PPh_3)_2$, Hoffmann et al.[3] have shown that the HOMO is a M–NO σ^* orbital and the LUMO a π^* orbital. Extended Hückel calculations showed that bending of the M–N–O angle away from 180° eases the σ^* antibonding interaction and significantly increases the π^* antibonding interaction while only slightly weakening the important π bonding interaction. The analogy with the present case seems quite clear, allowing us to predict that the SOMO in the radical anions of **1** and **3** is essentially M–NO σ^* with contributions from the metal a′ orbital and the nitrogen lone-pair orbital, and, if the M–N–O angle is bent away from 180°, the NO π^* orbital.

This picture of the electronic structure is indeed consistent with the ESR parameters. Consider first the g tensors. If the metal d-orbital contributions to the a′ and a″ orbitals are given by eq 8a and 8b, then substitution into eq 7 leads to the following contributions to **g**-tensor anisotropy from spin–orbit coupling of these orbitals:

$$g_x = g_e - (\lambda/\Delta)N_1^2N_2^2(R_1 - R_2)^2 \quad (9a)$$

$$g_y = g_e \quad (9b)$$

$$g_z = g_e - (\lambda/\Delta)N_1^2N_2^2(2 - R_1R_2)^2 \quad (9c)$$

where Δ is the (positive) energy difference between the a′ and a″ orbitals. In a C_{3v} complex with 90° L–M–L bond angles, the hybridization ratios R_1 and R_2 are both equal to $2^{1/2}$ and the **g**-tensor contributions of eq 9a and 9c both vanish. However, the ratios are very sensitive to bond angle, falling rapidly toward zero as the L–M–L angles increase from 90°. So long as there is approximate threefold symmetry about the metal, however, $R_1 \cong R_2$ so that the contribution to g_x is never expected to be significant. Unless the bond angles are very near 90°,[57] however, the contribution to g_z is expected to be substantial. There will be smaller positive contributions to all three **g**-tensor components through coupling of the SOMO with filled orbitals, but the major deviation from g_e is explained.

Furthermore, we can now identify g_3 ($g_\parallel$) with g_z and conclude that the major **g**-tensor axis is oriented toward the cyclopentadienyl ring.

If we assume an L–M–L bond angle of 95–100°, sufficient to explain the **g**-tensor anisotropy, then the M–N bond lies 122–118° away from the z axis, approaching the angle β which describes the orientation of the major **g** and ^{14}N hyperfine tensor axes. This suggests that the nitrogen 2p contribution is directed approximately toward the metal, consistent with the characterization of the SOMO as a metal–nitrogen σ^* orbital.

If the M–N–O bond angle were 180°, the only nitrogen contribution to the SOMO would be from the lone-pair orbital, an sp^n hybrid directed along the N–O bond axis. In nitrosyl complexes where the M–N–O angle is near 180°, ESR studies[21,48] have given a nitrogen p:s ratio between 1 and 2, consistent with this expectation. If the M–N–O angle is less than 180°, on the other hand, the nitrogen contribution to the SOMO should be a combination of the sp^n lone pair and π^* orbitals,[59] and the p:s ratio is expected to be larger (see Figure 7). In the present radicals, the p:s ratio is on the order of 10. To explain such a large p:s ratio, the bending must be quite substantial: a M–N–O angle of less than 130° is indicated.

A recent report[60] of the ESR spectrum of a radical believed to be $Mn(CO)_4NO^-$ provides a precedent for the interpretation given for the radical anions of **1** and **3**. The ESR spectrum of the manganese radical exhibited hyperfine coupling to both ^{55}Mn and ^{14}N and the major axes of both hyperfine tensors (as well as the **g** tensor) were colinear, uniquely defining the SOMO as a metal–nitrogen σ^* orbital composed of the Mn $3d_{z^2}$ orbital and N 2p orbitals equivalent to a 2p orbital oriented along the molecular z axis. Several arguments were presented for a bent Mn–N–O bond,[60] but most significantly for our purposes, the nitrogen 2s contribution to the SOMO is negligibly small.

Discussion

The ESR data establish that the reduction of $CpM(CO)_2NO$ involves a LUMO which is predominantly situated on the metal nitrosyl moiety. Furthermore, the reduced product has a severely bent nitrosyl group, a conclusion reached on the basis of the ESR parameters and the molecular orbital description of these complexes. Since the metal nitrosyl group is linear in the neutral complex (M–N–O angle of 178.9°),[61] the one-electron reduction of $CpM(CO)_2NO$ and the subsequent reoxidation of $CpM(CO)_2NO^-$ may be viewed as proceeding with a flipping of the nitrosyl group back and forth between the linear and bent forms. The exact angle for the bent nitrosyl cannot be specified, since the anions were too unstable to isolate for structural analysis, but the ESR data suggest that the M–N–O angle approaches that of sp^2 hybridization on nitrogen (<130°). Related 19-electron compounds, $CpW(NO)_2(PR_3)$, have recently been isolated after one-electron reduction of the precursor cations,[36] and X-ray data showed that the nitrosyl groups are only slightly bent (165.7° and 174.9°). In those radicals, the SOMO is distributed between the two NO groups, a conclusion reached similarly for the dinitrosyl dithiolate complexes of Mo and W.[20] Apparently, when the one-electron reduction is localized in a single M–N–O group the structural changes in the redox step are more severe.

If the structural change of the nitrosyl group occurs during the electron-transfer step, as seems likely, the quasi-reversibility of the redox couple may be ascribed at least in part to the increased activation barrier to electron transfer due to the energy required in the structural reorganization.[62] With use of a rate constant (uncorrected for potential distribution in the double layer) of $k_s = 10^{-2}$ cm/s, a free energy of activation to electron transfer of 7–8 kcal/mol is indicated. Since energy is also required to reorient solvent dipoles around the radical anion, this value may be viewed as an upper limit to flipping energy of the nitrosyl group during the electron-transfer reaction.

Bending of the nitrosyl group as a consequence of photochemical excitation of cyclopentadienyl metal nitrosyl compounds has been invoked to explain low-frequency bands (ca. 1390 cm^{-1}) observed during low-temperature matrix isolated photolysis of CpNi(NO) and $CpV(CO)(NO)_2$. The authors rationalized this behavior on the basis of charge transfer to the nitrosyl group.[63,64] Our observation that direct reduction of the nitrosyl group in **1** and **3** appears to result in bending of that substituent lends support to those assignments.

It is proper to raise the question of why the acetyl-substituted compound **2** has an $E°$ about 250 mV positive of that of the unsubstituted Cr compound **1**, if the redox orbital is predominantly metal nitrosyl based. It is clear that the acetyl group will exert an electron-withdrawing effect on the compound as a whole, and we take the shift in $E°$ to be simply an indication of the covalency of the metal–ligand bonds. A similar shift of 250 mV positive

(56) The nomenclature $\{MNO\}^n$ classifies the complex in terms of n, the total number of electrons associated with the metal d and the nitrosyl π^* orbitals, and makes no assumption about the actual distribution of valence electrons.[2]

(57) The average OC–Mn–CO bond angle in $CpMn(CO)_3$ is 92°: Berndt, A. F.; Marsh, R. E. *Acta Crystallogr.* **1963**, *16*, 118.

(58) McNeil, D. A. C.; Raynor, J. B.; Symons, M. C. R. *J. Chem. Soc.* **1965**, 410.

(59) The dipolar tensor expected for a linear combination of the two p orbitals, $ap_z + bp_x$, is still axial with the major axis oriented at $\theta = \tan^{-1}(b/a)$, i.e., the vector sum of the two p-orbital contributions.

(60) Lionel, T.; Morton, J. R.; Preston, K. F. *J. Phys. Chem.* **1982**, *86*, 367.

(61) Atwood, J. L.; Shakir, R.; Malito, J. T.; Herberhold, M.; Kremmitz, W.; Bernhagen, W. P. E.; Alt, H. G. *J. Organomet. Chem.* **1979**, *165*, 65.

(62) Marcus, R. A. *J. Chem. Phys.* **1965**, *43*, 679.

(63) Crichton, O.; Rest, A. J. *J. Chem. Soc., Dalton Trans.* **1977**, 986.

(64) Herberhold, M.; Kremnitz, W.; Trampisch, H.; Hitam, R. B.; Rest, A. J.; Taylor, D. J. *J. Chem. Soc., Dalton Trans.* **1982**, 1261.

has been reported, for example, in the oxidation of acetyl-substituted ferrocene, even though that oxidation involves an orbital which is mainly metal centered.[65] Substituent effects on $E°$ potentials may be a deceptive indicator of relative metal–ligand contributions to the redox orbital.[66]

Finally, a comparison may be made with the isoelectronic and isocharged complexes (η^6-arene)$Cr(CO)_3$. The latter reduce to dianions in a two-electron step which is chemically reversible if the arene is naphthalene. It is probable that the extra electrons in the chromium arene dianions are accommodated in an orbital mostly metal in character, and that the arene distorts to the tetrahapto form in the dianion to relieve the electronic strain on the metal.[67,68] It has been postulated that the arene distortion occurs after uptake of the first electron to give an intermediate which is actually electron deficient (17 e^- at the metal), leading directly to facile uptake of a second electron to give a 18 e^- metal in the dianion. Our nitrosyl analogue appears to avoid the necessity for a similar multielectron reduction by accommodating the extra electron in a predominantly nitrosyl-based orbital. There is a concomitant change in the M–N–O angle, but not necessarily in the mode of metal–polyolefin bonding (i.e., the M–Cp bond). Thus, the consequences to bonding of the metal–polyolefin unit are affected by the conceptual substitution of NO for CO, and they reflect the fact that the nitrosyl group is an effective "electron sink" in organometallic redox processes.

Acknowledgment. This work was generously supported by the National Science Foundation (CHE80-04242 and CHE83-03974) at the University of Vermont; acknowledgment is made to the donors of the Petroleum Research Fund, administered by the American Chemical Society, for partial support of this research at Brown University and at the University of Massachusetts. We also wish to thank Prof. Dennis Chasteen for obtaining the Q-band ESR spectrum.

Registry No. 1, 36312-04-6; **2**, 64539-47-5; **3**, 12128-13-1; $CpCr(CO)_2NO^-$, 92366-16-0; $CpMo(CO)_2NO^-$, 92396-57-1.

(65) Hoh, G. L. K.; McEwen, W. E.; Kleinberg, J. *J. Am. Chem. Soc.* **1961**, *83*, 3949.
(66) Geiger, W. E. In "Laboratory Techniques in Electrochemistry", Heineman, W., Kissinger, P. T., Eds.; Marcel Dekker: New York, Chapter 18.
(67) Rieke, R. D.; Arney, J. S.; Rich, W. E.; Willeford, B. R.; Poliner, B. S. *J. Am. Chem. Soc.* **1975**, *97*, 5951.
(68) Milligan, S. N.; Rieke, R. D. *Organometallics* **1983**, *2*, 171.

Mechanistic Features of C–H Activation by $ReH_7[P(C_6H_{11})_3]_2$

E. H. Kelle Zeiher, David G. DeWit, and Kenneth G. Caulton*

Contribution from the Department of Chemistry, Indiana University, Bloomington, Indiana 47405. *Received April 16, 1984*

Abstract: The synthesis and characterization of $ReH_7(PCy_3)_2$ (Cy = cyclohexyl) is reported. This compound is thermally resistant to the dimerization reaction exhibited by other $ReH_7(PR_3)_2$ compounds, which allows mechanistic features of C–H activation to be studied. Thus, in the temperature range 60–80 °C, $ReH_7(PCy_3)_2$ exchanges hydrogen with deuteriobenzene. Deuterium is incorporated into the complex not only as hydride ligands but also selectively at the C2 and C3 carbons of all cyclohexyl rings. Only one of the two methylene hydrogens at each of these carbons is exchangeable. It is also shown that exchange at the two adjacent carbons does *not* proceed by concerted dehydrogenation via a cyclohexenyl intermediate; the rate of deuterium incorporation at C3 differs from that at C2. On the basis of observation of exchange with D_2, and also kinetic studies of the reaction of $ReH_7(PCy_3)_2$ with phosphine and olefinic nucleophiles, all of the thermal reactions observed here are concluded to arise from the reductive elimination transient $ReH_5(PCy_3)_2$.

The majority of neutral phosphine polyhydride complexes $(MH_x(PR_3)_y$, $x \geq 3)$ of the second and third transition series metals are coordinatively saturated and relatively unreactive. We have reported that photolysis of several coordinatively saturated (18 electron) transition-metal polyhydride phosphine complexes leads (by H_2 or phosphine photodissociation) to transients of high reactivity toward olefins, CO, Lewis bases, and even saturated hydrocarbons.[1-3] It is our objective to broaden the utility of polyhydride complexes by making them susceptible to thermal activation (cf. $OsH_4(PMe_2Ph)_3$,[3] which may be quantitatively recovered after 24 h at 100 °C).

The approach described here has been to incorporate a particularly bulky phosphine ligand into the complex in order to promote (phosphine?) ligand dissociation or perhaps even the isolation of a 16-electron complex. Our flash photolysis study[4] of $ReH_5(PMe_2Ph)_2$, which is the reactive transient in our photochemistry derived from $ReH_5(PMe_2Ph)_3$, gave evidence for undesirable stabilization of this phototransient by an aryl ring attached to the phosphine ligand. Additionally, in another case we have isolated a product of aryl ring orthometalation.[2] Consequently, we decided to avoid aryl phosphines altogether. We report here on results using tricyclohexyl phosphine which confirm a thermal route to ligand dissociation and permit rather detailed examination of the reactivity of the resulting 16-electron transient. Intramolecular attack on aliphatic C–H bonds has been observed to occur via a 16-electron Re(V) complex.

Experimental Section

General. All manipulations were carried out under N_2 with use of standard Schlenk and glove box techniques. Benzene, toluene, cyclohexane, and THF were vacuum transferred from sodium benzophenone

(1) Green, M. A.; Huffman, J. C.; Caulton, K. G. *J. Am. Chem. Soc.* **1981**, *103*, 695.
(2) Green, M. A.; Huffman, J. C.; Caulton, K. G.; Rybak, W. K.; Ziolkowski, J. J. *J. Organomet. Chem.* **1981**, *218*, C39.
(3) Green, M. A.; Huffman, J. C.; Caulton, K. G. *J. Organomet. Chem.* **1983**, *243*, C78.
(4) Muralidharan, S.; Ferraudi, G.; Green, M. A.; Caulton, K. G. *J. Organomet. Chem.* **1983**, *244*, 47.

0002-7863/84/1506-7006$01.50/0